Quasi-γ band in ^{114}Te

Prithwijita Ray, H. Pai,[*] Sajad Ali,[†] Anjali Mukherjee, and A. Goswami[‡]
Saha Institute of Nuclear Physics, 1/AF Bidhan Nagar, Kolkata 700064, India and Homi Bhabha National Institute, Training School Complex, Anushaktinagar, Mumbai 400094, India

S. Rajbanshi
Department of Physics, Presidency University, Kolkata 700073, India

Soumik Bhattacharya, R. Banik, S. Nandi, S. Bhattacharyya, G. Mukherjee, and C. Bhattacharya
Variable Energy Cyclotron Centre, 1/AF Bidhan Nagar, Kolkata 700064, India and Homi Bhabha National Institute, Training School Complex, Anushaktinagar, Mumbai 400094, India

S. Chakraborty
Nuclear Physics Group, Inter-University Accelerator Centre, New Delhi 110067, India

G. Gangopadhyay
Department of Physics, University of Calcutta, Kolkata 700009, India

Md. S. R. Laskar and R. Palit
Department of Nuclear and Atomic Physics, Tata Institute of Fundamental Research, Mumbai 400005, India

G. H. Bhat and S. Jehangir
Department of Physics, Sri Pratap College, Srinagar 190001, India and Cluster University Srinagar, Jammu and Kashmir, 190001, India

J. A. Sheikh
Cluster University Srinagar, Jammu and Kashmir, 190001, India and Department of Physics, University of Kashmir, Srinagar 190006, India

A. K. Sinha
UGC-DAE Consortium for Scientific Research, University Campus, Khandwa Road, Indore 452017, India

S. Samanta, S. Das, S. Chatterjee, R. Raut, and S. S. Ghugre
UGC-DAE Consortium for Scientific Research, Kolkata Centre, Kolkata 700098, India

(Received 3 August 2019; revised manuscript received 14 May 2020; accepted 2 June 2020; published 15 June 2020)

The low-lying non-yrast states in ^{114}Te have been investigated using the Indian National Gamma Array through the fusion-evaporation reaction ^{112}Sn(^{4}He, $2n$) at a beam energy of 37 MeV. Eight new γ transitions have been placed in the level scheme to establish the quasi-γ band in this nucleus. Spin and parity of several excited states have been assigned from the present spectroscopy measurements. The comparison of experimental results on the observed bands with the interacting boson model (IBM) and triaxial projected shell model (TPSM) confirms the existence of the quasi-γ band structure in the ^{114}Te nucleus.

DOI: 10.1103/PhysRevC.101.064313

I. INTRODUCTION

A large number of collective and noncollective states have been observed at lower excitation energies, exhibiting a shape coexistence mainly caused by proton 2p-2h excitation along with the spherical ground states across the $Z = 50$ shell closure. For deformed nuclei, the nuclear shapes have traditionally been described in terms of β and γ parameters, where the

[*]h.pai@saha.ac.in; hari.vecc@gmail.com
[†]Government General Degree College at Pedong, Kalimpong, 734311, India.
[‡]Deceased.

former specifies the ellipsoidal quadrupole deformation and the latter the degree of axial asymmetry. The most common low-lying collective excitation, namely γ vibration, has been extensively reported in several mass regions throughout the nuclear chart over decades [1–4]. γ bands are associated with ellipsoidal oscillation of nuclear shape. This kind of phenomenon is favorable when the potential energy surfaces are found to be soft for both β and γ deformation parameters, ensuring that shape polarization can take place.

In the last decade, several groups have tried to tackle the question of whether the pure vibrational structure can or cannot be observed in the nuclei in the $Z \approx 50$ region. In this context, the work by Garret and Wood is useful to understand the interplay between γ-soft and vibrational character of the low-lying collective excitations in these nuclei [5]. Consequently, the quasi-γ bands and coexistence of different nuclear shapes associated with intruder configuration at low angular momentum were observed frequently in these nuclei [6–10]. Recently, a γ band built on the shape-coexisting intruder configuration was reported in Cd isotopes [11]. Well-developed quasi-γ bands, built on the 2_2^+ state, were reported in even-even Xe and Ba isotopes, having both favored and unfavored partners [4,12]. The ^{120,122,124}Te nuclei were reported to be soft triaxial in nature [13] and hence the occurrence of quasi-γ bands is also expected in these nuclei. Consequently, the quasi-γ bands have been identified recently in heavier mass ^{124,126}Te isotopes, but without any in-band γ transitions [14]. However, the quasi-γ bands have not been studied well in any of the lighter mass Te isotopes. Only the favored partner of the quasi-γ band was reported tentatively in ^{118}Te [15]. As the excitation energy of the quasi-γ vibrational states is sensitive to a different kind of critical point symmetry [16–18], it is important to search for the quasi-γ bands in Te isotopes systematically to investigate the shape evolution of Te nuclei. With this motivation, an attempt has been made to search for the quasi-γ band in ^{114}Te.

The low-lying non-yrast structure of neutron deficient ^{114}Te has not been studied extensively. Only a few experimental studies have been reported [19–21]. This nucleus is shown to mimic the U(5) dynamical symmetry based on the energy ratio $R_{4/2}$ of 2.09. However, the transition probabilities [$B(E2)$], extracted from the lifetime measurement, are found to be in strong contradiction with the same estimated by theoretical interacting boson model (IBM) within the U(5) limit [22,23]. In this context, it is worth noting that a reasonable description of the yrast $B(E2)$ values was reported recently from a large-scale shell-model study [24]. In order to elucidate the underlying structure of ^{114}Te, an experiment was carried out using an α beam, delivered by the K-130 cyclotron of the Variable Energy Cyclotron Centre, Kolkata.

II. EXPERIMENTAL DETAILS

The excited states in ^{114}Te were populated through the fusion-evaporation reaction ^{112}Sn(^{4}He, $2n$) ^{114}Te at a beam energy of 37 MeV delivered by the K-130 cyclotron accelerator of the Variable Energy Cyclotron Centre, Kolkata. A self-supporting isotopically enriched (99.6%) ^{112}Sn foil of effective thickness 4.5 mg/cm^2 was used as a target [25]. The deexcited γ rays were detected by the Indian National Gamma Array (INGA), stationed at the Variable Energy Cyclotron Centre, Kolkata, comprising seven Compton-suppressed HPGe (high purity germanium) clover detectors and one LEPS (low energy photon spectrometer) detector [26]. These detectors were arranged at different angles (θ) with respect to the beam direction; four clover detectors at $\theta = 90^\circ$ (two in plane and two out of plane), two clover detectors at $\theta = 125^\circ$, one clover detector at $\theta = 40^\circ$, and the LEPS detector at $\theta = 40^\circ$. The energy and efficiency calibrations were performed using ^{133}Ba and ^{152}Eu radioactive sources placed at the target position of the INGA setup.

The pulse processing and data acquisition system was based on PIXIE-16 12-bit 250 MHz digitizer modules manufactured by XIA LLC and running on firmware conceptualized by UGC-DAE CSR, Kolkata Centre [27]. Time stamped list mode data was acquired with event trigger generated from coincidence firing of at least two Compton suppressed clover detectors. Around 1.5×10^8 such events were acquired during the experiment. The data were processed into spectra, $\gamma\gamma$ matrices, and $\gamma\gamma\gamma$ cube using the IUCPIX [27,28] package, developed at UGC-DAE CSR, Kolkata Centre, and analysed using RADWARE [29] and INGASORT [30] packages.

III. DATA ANALYSIS PROCEDURES

The spin of an excited nuclear state can be determined from the multipolarity of the γ ray. The multipolarities of the γ-ray transitions were determined from the angular correlation analysis using the method of directional correlation from the oriented states (DCO) ratio [31]. For the DCO ratio analysis, an asymmetric matrix was constructed using the coincidence events registered in the detectors placed at angles 125° and 90° with respect to the beam axis. The DCO ratio of the γ-ray transition (γ_1) at angle $\theta_1 = 125^\circ$ gated by the transition of known multipolarity (γ_2) at angle $\theta_2 = 90^\circ$ is defined as

$$R_{\rm DCO} = \frac{I_{\gamma_1} \text{ at } \theta_1,\ \text{gated by } \gamma_2 \text{ at } \theta_2}{I_{\gamma_1} \text{ at } \theta_2,\ \text{gated by } \gamma_2 \text{ at } \theta_1}. \tag{1}$$

For the same multipolarity of the stretched transitions γ_1 and γ_2, the value of $R_{\rm DCO}$ is close to unity. The value of $R_{\rm DCO}$ for the transitions γ_1 and γ_2 with different multipolarities depends on the detector angles (θ_1 and θ_2) and the mixing ratios (δ) associated with the transitions. The validities of the measured $R_{\rm DCO}$ values were checked with the known transitions in ^{114}Te [21] and have been compared with the theoretical values calculated using the code ANGCOR [32]. In the present geometry, the calculated value of $R_{\rm DCO}$ [32] for a pure dipole (quadrupole) transition gated by a stretched quadrupole (dipole) transition is 0.70 (1.50). Measured experimental values for the pure dipole (936.2 keV, $7^- \rightarrow 6^+$, $E1$) and quadrupole (774.8 keV, $4^+ \rightarrow 2^+$, $E2$) transitions of ^{114}Te are 0.70 (0.08) and 1.60 (0.18), respectively, in good agreement with the calculated values [32]. The width of the substate population (σ/J) required for the $R_{\rm DCO}$ calculation is assumed to be of 0.37 for the present experiment.

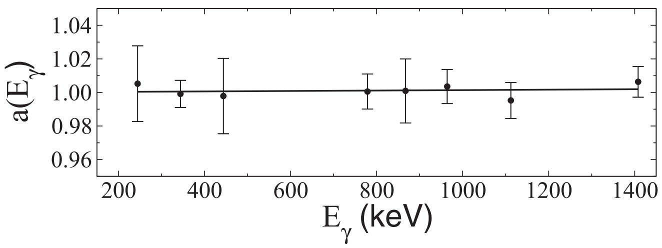

FIG. 1. The asymmetry correction factor $a(E_\gamma)$ at different γ-ray energies from a ^{152}Eu source. The solid line corresponds to a linear fit of the data.

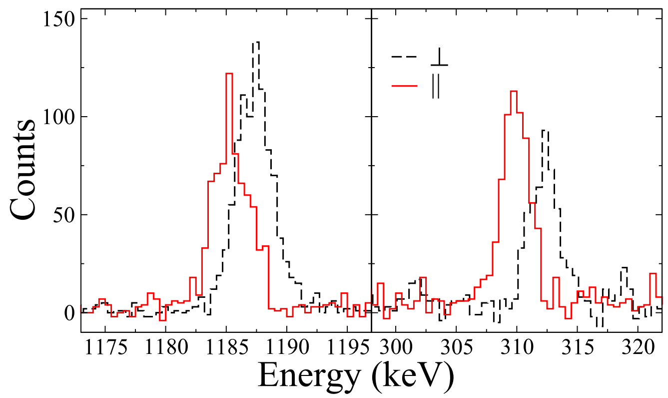

FIG. 2. The perpendicular (black dashed line) and parallel (red solid line) components of the two γ rays in ^{114}Sb, obtained from the linear polarization analysis in the present work. The 309.2 keV transition (right) is known as a magnetic type transition whereas the 1184.9 keV transition (left) is an electric type transition. The perpendicular component was shifted in energy for clarity.

Definite parities of the excited states have been designated from the linear polarization asymmetry ratio (Δ_{asym}), extracted from the parallel and perpendicular scattering of the γ photons inside the detector medium [33–35]. The measured value of Δ_{asym} provides a qualitative idea about the electric or magnetic nature of the transitions. The Δ_{asym} value for a γ transition was deduced using the relation

$$\Delta_{\text{asym}} = \frac{a(E_\gamma)N_\perp - N_\parallel}{a(E_\gamma)N_\perp + N_\parallel}, \tag{2}$$

where $N_\parallel$ and $N_\perp$ are the counts for the actual Compton-scattered γ rays in the planes parallel and perpendicular to the reaction plane, respectively. Correction due to the asymmetry

TABLE I. Initial states (E_i) and energies of γ rays (E_γ), relative intensity (I_γ), DCO ratios (R_{DCO}), linear polarization asymmetry (Δ_{asym}), mixing ratio (δ), and deduced multipolarity ($E\lambda/M\lambda$) of the γ transitions in ^{114}Te.

E_i (keV)	E_γ (keV)[a]	I_γ[b]	J_i^π	J_f^π	R_{DCO}	Δ_{asym}	δ	$E\lambda/M\lambda$
708.7	708.7	100.0(5.2)	2^+	0^+	1.00(0.08)[f]	+0.12(0.01)		$E2$
1348.2	639.5	0.33(0.05)	$(0)^{+}$[c]	2^+	0.94(0.45)[d]			$(E2)$
1391.2	682.3	9.28(0.94)	2^+	2^+	0.96(0.11)[d]	−0.07 (0.03)	2.5	$M1+E2$
	1391.2	0.12(0.03)	2^+	0^+				
1483.5	774.8	84.7(8.6)	4^+	2^+	0.98(0.11)[d]	+0.13(0.01)		$E2$
1794.7	310.9	1.00(0.11)	3^+	4^+	0.63(0.08)[d]		3.0	$M1+E2$
	403.1	0.80(0.08)	3^+	2^+	0.56(0.08)[d]			$M1+E2$
	1086.1	4.11(0.42)	3^+	2^+	0.82(0.10)[d]	+0.01(0.04)	0.29	$M1+E2$
2026.9	543.3	1.56(0.17)	4^+	4^+	0.83(0.11)[d]	−0.11 (0.09)	2.2	$M1+E2$
	635.5	7.17(0.72)	4^+	2^+	1.00(0.11)[e]	+0.14 (0.02)		$E2$
	1318.3	0.85(0.10)	4^+	2^+	0.99(0.16)[d]			$E2$
2217.2	733.7	74.2(7.6)	6^+	4^+	0.98(0.11)[d]	+0.12(0.01)		$E2$
2450.1	655.3	3.93(0.40)	5^+	3^+	0.97(0.11)[d]	+0.05(0.04)		$E2$
	967.0	0.56(0.10)	5^+	4^+	0.58(0.12)[d]		−3.8	$M1+E2$
2645.1	618.1	4.11(0.42)	6^+	4^+	0.98(0.11)[d]	+0.23(0.07)		$E2$
	1162.1	0.57(0.07)	6^+	4^+	0.96(0.16)[d]	+0.44(0.21)		$E2$
2694.7	1210.7	0.43(0.1)	(4^+)	4^+				$(M1+E2)$
	1303.7	0.25(0.04)	(4^+)	2^+	0.91(0.27)[d]			$(E2)$
3084.7	634.6	2.14(0.26)	7^+	5^+	0.88(0.12)[f]	+0.06 (0.03)		$E2$
3088.4	871.2	33.5(3.4)	8^+	6^+	0.98(0.11)[d]	+0.12(0.01)		$E2$
3504.5	859.5	0.27(0.04)	8^+	6^+	0.93(0.14)[e]	+0.07(0.06)		$E2$
	1287.0	0.40(0.15)	8^+	6^+				$(E2)$
3909.7	825.0	0.95(0.11)	9^+	7^+	0.91(0.14)[d]	+0.11(0.06)		$E2$

[a]Uncertainty in γ-ray energy is ± (0.3–0.5) keV.
[b]Intensities of γ rays are normalized to the 708.7 keV transition, with $I_\gamma = 100$. Intensity uncertainties does include the errors due the uncertainty in efficiency correction.
[c]From Ref. [37].
[d]DCO ratios are obtained from 708.7 keV stretched quadrupole ($E2$) transition.
[e]DCO ratios are obtained from 618.1 keV stretched quadrupole ($E2$) transition.
[f]DCO ratios are obtained from 774.8 keV stretched quadrupole ($E2$) transition.

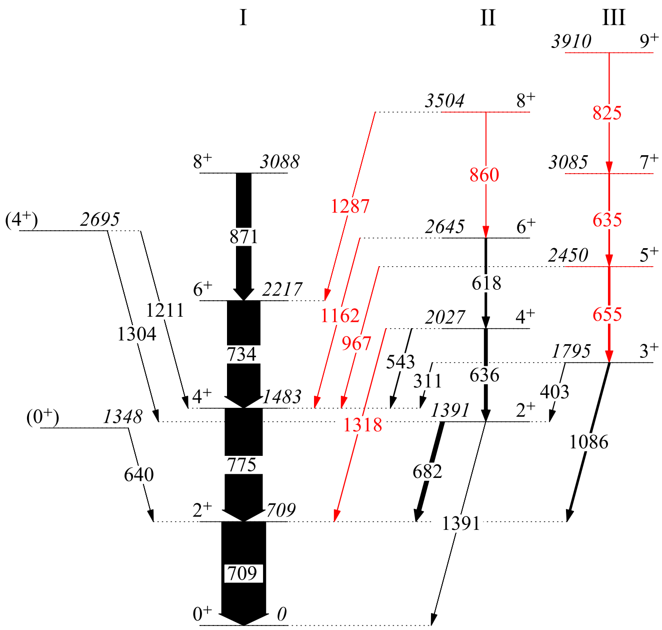

FIG. 3. Partial level scheme of ^{114}Te, deduced from this work. Newly identified γ rays and levels are marked in red (gray) color.

in the array and the response of the clover segments, defined by $a(E_\gamma) = \frac{N_\parallel}{N_\perp}$, was estimated using an unpolarized ^{152}Eu source. The energy dependence of the parameter $a(E_\gamma)$ is obtained using the expression $a(E_\gamma) = a + b(E_\gamma)$. The fitting, shown in Fig. 1, gives the values of the constants as $a = 1.000(3)$ and $b(E_\gamma) \approx 10^{-6}$. A positive value of $\Delta_{\rm asym}$ indicates an electric (E) type transition, whereas a negative value indicates a magnetic (M) type transition. The low energy cutoff for the polarization measurement in the present work was about 200 keV. The validity of this method has been confirmed from the known transitions of energy 1184.9 and 309.2 keV in ^{114}Sb (Fig. 2) which were also produced in the same experiment [36,37].

IV. EXPERIMENTAL RESULTS

The low-lying level scheme of ^{114}Te (up to $E_x \approx 4$ MeV) has been updated in the present work by placing eight new γ transitions as shown in Fig. 3. Energy levels were grouped into three bands, I–III. The experimental results obtained in the present work are summarized in Table I. Measured relative intensities of the γ rays from the single-gated spectra were normalized for the 708.7-keV transition. Relevant energy-gated $\gamma\gamma$ spectra in support of the present placements are presented in Figs. 4–7. These spectra show the previously reported γ rays in ^{114}Te [19–21] along with the newly observed γ rays.

A. Band I

Band I, earlier reported up to $I^\pi = 8^+$ at 3089 keV [20,21,23], is a positive parity band built on the ground state configuration. All the previously reported transitions of this band have been identified in the present work. Spins and parity of the states have been adopted from Ref. [20,23] after verification from the present spectroscopic results.

B. Band II

A sequence of two γ rays marked as band 5 in Ref. [20] was reported up to $E_{(6^+)} = 2644$ keV with tentative spin and parity assignment. This sequence, which is found to decay to the ground state band via 682.3 ($\Delta I = 0$) and 1391.2 ($\Delta I = 2$) keV γ rays, has been extended further up to $E_{8^+} = 3504.5$ keV by placing a 859.5 keV γ ray. Another nearby 8^+ state at 3505.5 keV [20], reported earlier, decays to the $I^\pi = 6^+$ state at 2217.2 keV via 1289.8 keV γ transition. In this work, another decay branch of this state to the $I^\pi = 6^+$ state at 2645.1 keV via 862.3 keV γ transition has been identified. Observation of the both 859.5 and 862.3 keV transitions in the 618.1 keV energy gate and only an 862.3 keV transition in the 412.2 keV (3918.7 keV → 3505.5 keV [20]) energy gate confirm these placements (Fig. 6). In a similar fashion, energy gates of 412.2 and 733.7 keV can serve the purpose for the 1289.8 and 1287.0 keV transitions, as shown in Fig. 6. The 3504.5 keV state is found to decay into bands I and II mainly via 1287.0 and 859.5 keV transitions. However, the 3505.5 keV state is found to decay into the 2605.8 keV state [20] more intensely via 900.7 keV transition than the 1289.8 or 862.3 keV transition, as observed from the 412.2 keV energy gate. Therefore, the 3504.5 keV state is considered as a member of the band II. Three new $\Delta I = 2$ γ transitions, viz.,

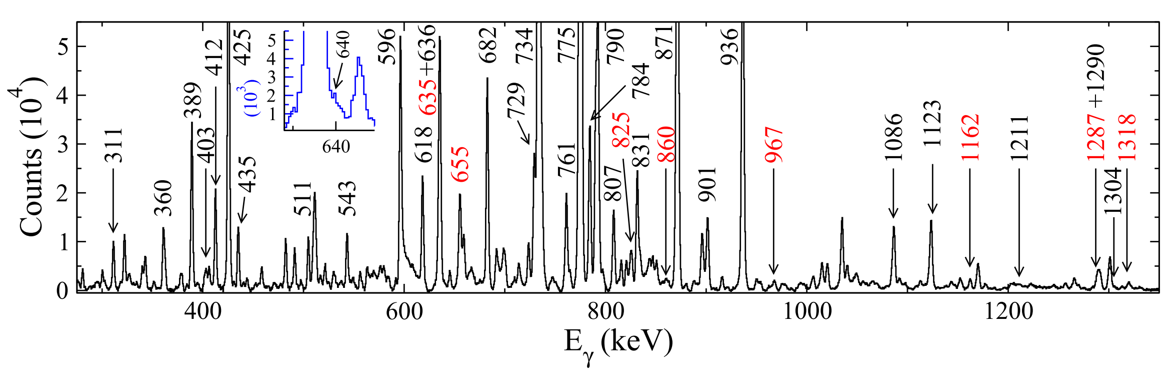

FIG. 4. Spectrum to show the γ rays observed in coincidence with the 708.7 keV γ transition in ^{114}Te. Newly observed γ rays are shown in red (gray) color. γ rays that are marked here but not included in Fig. 3 were already reported in Ref. [20].

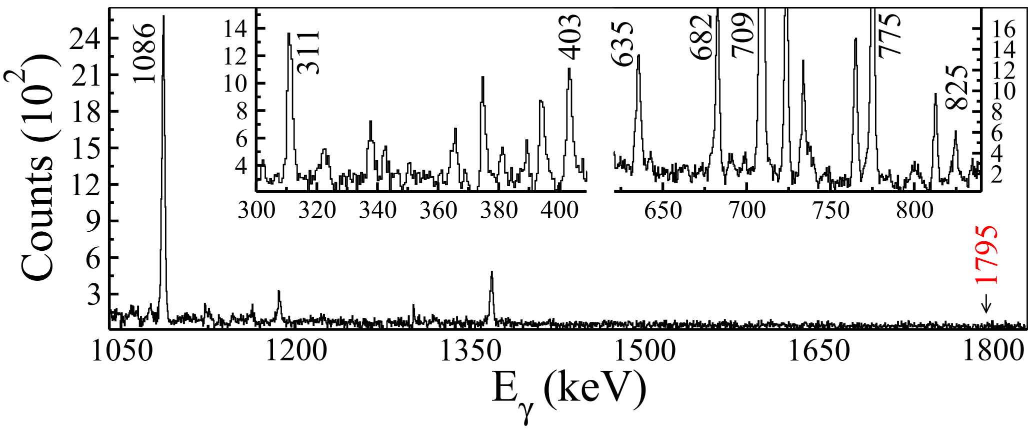

FIG. 5. Prompt $\gamma\gamma$ coincidence spectra gated by 655.3 keV transition. The 1795 keV (red marked) transition was reported in Refs. [37,38], but not observed in the present work.

1318.3 ($4_2^+ \rightarrow 2_1^+$), 1162.1 ($6_2^+ \rightarrow 4_1^+$), and 1287.0 ($8_2^+ \rightarrow 6_1^+$) keV, have been placed in the level scheme. The energy gated spectrum of 708.7 keV is presented in Fig. 4, in favor of the present placement. Spin and parity of all the states belonging to this band have been assigned on the basis of present spectroscopic results. Both the $\Delta I = 0$ transitions, viz., 543.3 and 682.3 keV, were found to have significant $E2$ admixture as estimated from the mixing ratio extracted from the present DCO ratio (Table I).

C. Band III

A state at 1794.7 keV, decaying mainly to the $I^\pi = 2^+$ state at 708.7 keV via 1086.1 keV γ transition, was reported with a tentative spin-parity $I^\pi = (2^+)$ assignment from the β^+ decay study of the ^{114}I [37,38]. Apart from this strongest decay branch, this state was reported to decay via another three branches via 310.7, 403.0, and 1793.4 keV γ transitions [37,38]. Three (viz., 310.9, 403.1, and 1086.1 keV) out of these four decay paths have also been identified in the present work (Fig. 5). The experimental DCO ratio of these three transitions supports present $I^\pi = 3^+$ assignment for this state. According to the present spin-parity assignment, the multipolarity of the 1795 keV transition becomes $\Delta I = 3$, which may be one of the causes for nonobservation of this transition in this study. The available branching ratio of the 1795 keV state also indicates a very low intensity ($I_\gamma \approx 0.4$) of this transition, which is again beyond the present detection limit. A sequence of three γ transitions, viz., 655.3, 634.6, and 825.0 keV (marked as band III), has been established above this 1794.7 keV state on the basis of $\gamma\gamma$ coincidence study. The 708.7 and 655.3 keV energy gated spectra are shown, in favor of the present placement (Figs. 4 and 5). Spin and parity of all the states belonging to this sequence have been assigned firmly on the basis of angular correlation and linear polarization results, as listed in Table I.

D. Other non-yrast states

Apart from the above mentioned groups of states (bands I–III), two more excited states at 1348.2 and 2694.7 keV have also been observed in this work and are related to the present interest. These two states were reported earlier in a β^+ decay study of ^{114}I [38]. The 1348.2 (2694.7) keV state with $I^\pi = (0^+)$ ($I^\pi = (4^+)$) was found to decay to the 708.7 (1483.5/1391.2) keV state(s) via 639.5 (1210.7/1303.7) keV γ transition(s). Energy gated spectra of 639.5, 1210.7, and 1303.7 keV γ transitions are shown in Fig. 7, to confirm these placements. The DCO ratios of 639.5 and 1303.7 keV γ transitions indicate the quadrupole nature of these transitions.

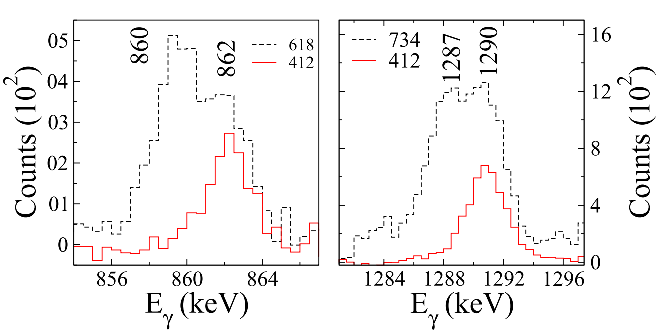

FIG. 6. Prompt $\gamma\gamma$ coincidence spectrum of (left) 618 and 412 keV and (right) 734 and 412 keV transitions.

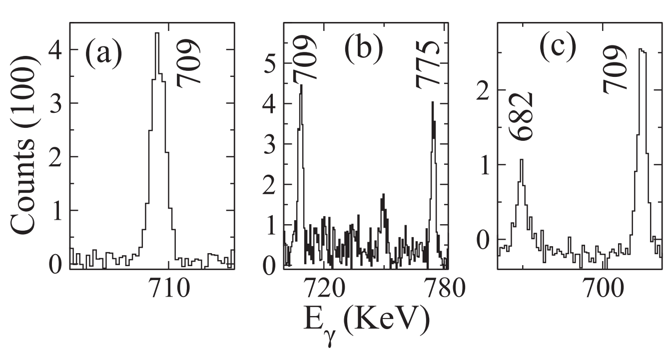

FIG. 7. Prompt $\gamma\gamma$ coincidence spectra gated by (a) 639.5 keV, (b) 1210.7 keV, and (c) 1303.7 keV transitions.

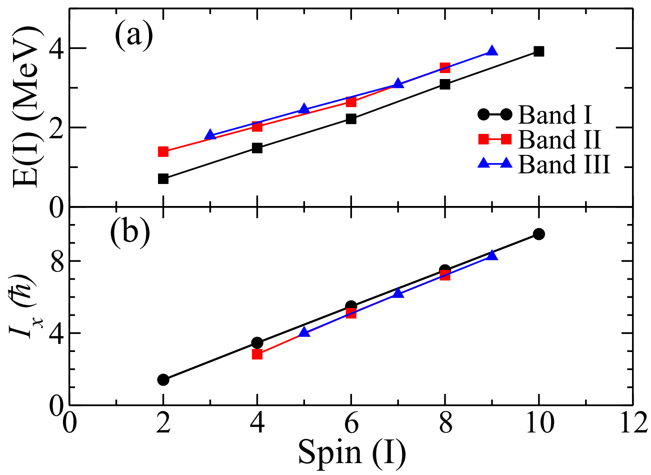

FIG. 8. (a) The experimental excitation energies of bands I, II, and III vs spin. (b) Projection of total angular momentum on the rotation axis (I_x) of band I, II, and III plotted vs spin.

V. DISCUSSION

The low-lying structure of ^{114}Te mainly consists of three sequences of $E2$ transitions. Apart from the strongly populated ground state band (I), two more band structures were established in the present work. The excitation energy and the projection of the total angular momentum on the rotation axis (I_x) of these bands are plotted vs spin, as shown in Figs. 8(a) and 8(b). The excitation energy and I_x versus spin plots show similar slopes for the ground-state band (band I) and the other two bands (bands II and III), indicating that the dynamic moment of inertia of these bands is nearly equal. Coupling of a phonon excitation with a rotational configuration can give rise to a similar moment of inertia [39,40]. Therefore, similar characteristics for all the three bands indicate that bands II and III correspond to the quasi-γ vibrational structure. The properties of $\Delta I = 0$ transitions, as pointed out in Refs. [4,12], are also found to be consistent in the present case. The $E2$ fractions of $2^+_1 \rightarrow 2^+_2$ and $4^+_1 \rightarrow 4^+_2$ $\Delta I = 0$ transitions are found to be decreasing with increasing spin. The odd-even energy staggering [$S(I)$] [17,18] plotted as a function of spin also shows a similar pattern when compared with the quasi-γ band of ^{118}Xe (as shown in Fig. 9), with the minimum at even spin indicating the band structure observed in ^{114}Te is

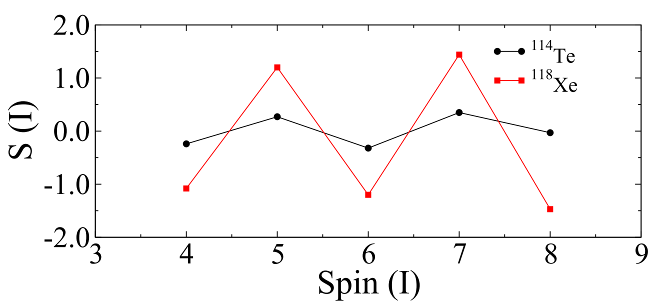

FIG. 9. Calculated odd-even energy staggering $S(I)$ plotted against spin (I) for ^{114}Te. Values for ^{118}Xe are taken from literature [41,42].

of quasi-γ vibrational nature. However, the absolute values of staggering are small in the present case compared to ^{118}Xe [17,41,42]. The calculated value of $E_s/E(2^+_1)$ is -0.13 which indicates a γ-soft nature for the nucleus [43].

The experimental results are discussed below in the light of both interacting boson model (IBM) and triaxial projected shell model (TPSM) calculations.

A. Interacting boson model approximation

Nuclei in the neighborhood of $Z = 50$ shell closure are known to be anharmonic vibrators and hence are expected to be close to the U(5) limit of the interacting boson model (IBM). For example, Van Ruyven *et al.* [15] found that excited states in ^{118,120}Te can be very well understood in terms of IBM. Ground bands of Sn nuclei have been described by U(5) symmetry [44].

However, there is evidence that significant departure from the U(5) symmetry is also possible in some of the nuclei in this region. Cd nuclei with $Z = 48$ can be described by a U(5) as well as a non-U(5) Hamiltonian [45]. Möller *et al.* [23] have studied the excited states and the electromagnetic transition probabilities in ^{114}Te. They concluded that, though the ground band can be explained well in terms of the U(5) limit of IBM, it fails to explain the trend of the $B(E2)$ values.

Here, the yrast band of ^{114}Te is known up to the 8^+ state. Though this band can be easily described by the U(5) model, we found that the quasi-γ vibrational band predicted by this model shows strong staggering, in disagreement with experimental data. For this reason, we decided to use a more general IBM-1 Hamiltonian. Since the number of bosons is not too large and the ground band is easily described by the U(5) limit of the Hamiltonian, we considered a Hamiltonian which has an additional quadrupole-quadrupole interaction consistent with the O(6) limit. A similar Hamiltonian was used by McCutchan *et al.* [17] in their study on Ba, Xe, and Ce isotopes. The two-parameter Hamiltonian they used was

$$H = C\left[(1-\zeta)n_d - \frac{\zeta}{4N_B}Q^\chi \cdot Q^\chi\right] \tag{3}$$

where

$$n_d = (d^\dagger\tilde{d})_0, \quad Q^\chi = (d^\dagger\tilde{s})_2 + (s^\dagger\tilde{d})_2 - \chi(d^\dagger\tilde{d})_2, \tag{4}$$

written in terms of the d boson creation and annihilation operators [46]. The two parameters are C and ζ, and N_B is the number of bosons. the parameter χ was not taken as free. In the U(5) limit, the second term is absent. In the O(6) limit, $\chi = 0$ and the first term does not occur. Saxena *et al.* have also used a similar Hamiltonian for IBM-2 [13] to describe heavier Te isotopes where they have varied the value of χ. In accordance with O(6) symmetry, we chose χ as zero and treated the coefficients of the other two terms as free parameters. We fitted the excitation energies by minimizing the sum of errors in energy prediction to extract the parameters. However, our results were not very satisfactory. We then decided to extend our Hamiltonian by adding another term,

$$L = \sqrt{10}(d^\dagger\tilde{d})_1, \tag{5}$$

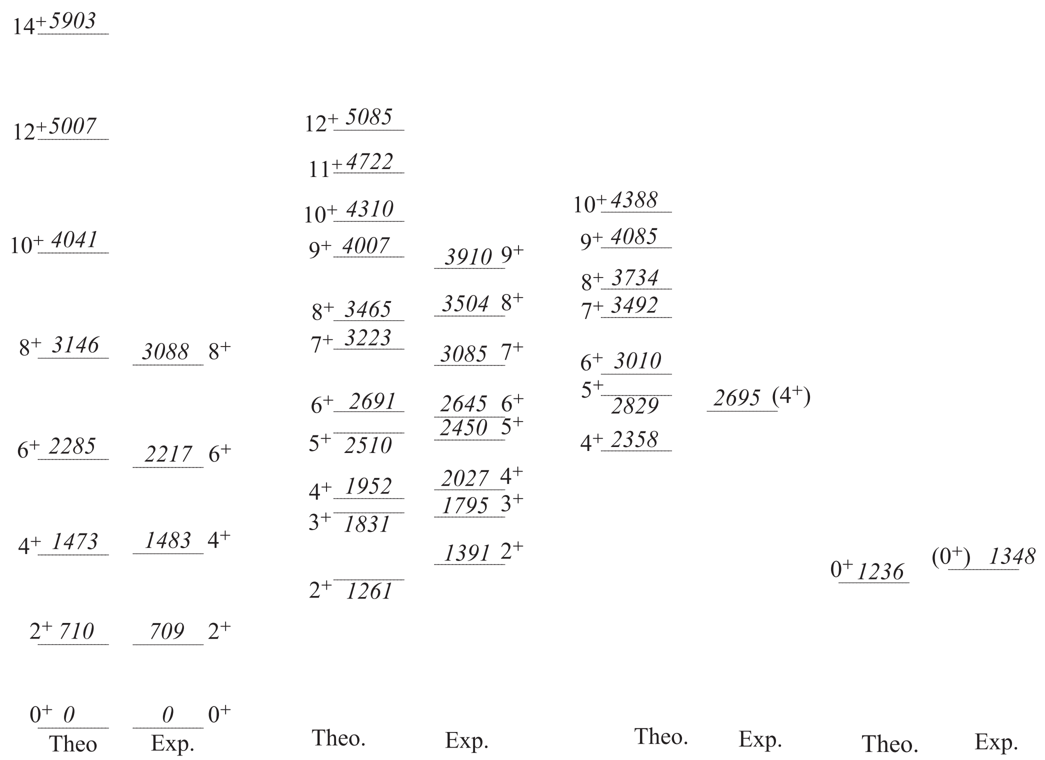

FIG. 10. Comparison of experimental and calculated band energies using the IBM formalism in ^{114}Te. The level energies associated with the states are given in keV.

so that our Hamiltonian can be written as

$$H = \epsilon n_d + a_1(L \cdot L) + a_2(Q \cdot Q). \tag{6}$$

The parameters obtained after fitting are $\epsilon = 0.497$ MeV, $a_1 = 0.02548$ MeV, and $a_2 = 0.042$ MeV. The rms deviation for fourteen excited states is 117.63 keV. The result of the three-parameter fitting is shown in Fig. 10. As one can see, the agreement is reasonably good. The coefficient of the quadrupole-quadrupole interaction term is of typical magnitude and has a significant effect on the staggering in the quasi-γ vibrational band. Hence, we may conclude that this nucleus falls between the U(5) and the O(6) symmetries. Furthermore, we see that the ratio of the excitation energy values of the first 4^+ state to the first 2^+ state has the value 2.09. Similarly, the ratio of the energy of the quasi-γ bandhead to that of the first 2^+ state is 1.96. These values, along with the results of the calculation, indicate that the nucleus ^{114}Te lies between the vibrator and the E(5) critical point of the Casten symmetry triangle [16] on the arm connecting the U(5) and the O(6) dynamical symmetries.

It is possible to further specify the position of the Hamiltonian on the symmetry triangle. Casten *et al.* have mapped the symmetry triangle of the IBM Hamiltonian in [47] where they have introduced radial coordinates (ρ, θ) spanning the symmetry triangle. In this notation U(5) symmetry corresponds to $\rho = 0$; SU(3) to $\rho = 1$, $\theta = 0$; and O(6) to $\rho = 1$, $\theta = \pi/3$. This allows one to specify the place of the IBA Hamiltonian in the symmetry triangle. In our case, we have considered the parameter χ in Eq. (4) to be zero, hence $\theta = \pi/3$. A calculation involving the values of the two parameters n_d and a_2 in Eq. (6) yields $\rho = 0.70$. Thus we may conclude that the nucleus lies on the arm connecting the U(5) and the O(6) symmetries, relatively closer to the latter.

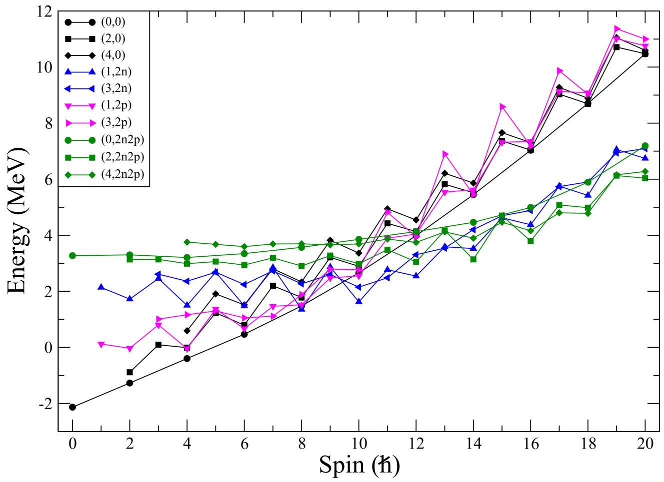

FIG. 11. Theoretical band diagram for ^{114}Te. The labels $(K, \#)$ characterize the states, with K denoting the K quantum number and # the number of quasiparticles. For example, (0,0), (2,0), and (4,0) correspond to the $K = 0$ ground-state band, the $K = 2$ γ band, and the $K = 4$ $\gamma\gamma$ band, respectively, projected from the 0-qp state. $(1, 2n)$, $(3, 2n)$, $(1, 2p)$, $(3, 2p)$, (2,4), and (4,4) correspond, respectively, to the projected two-neutron aligned state, two-proton aligned state, and two-neutron plus two-proton aligned state, with different quantum numbers K.

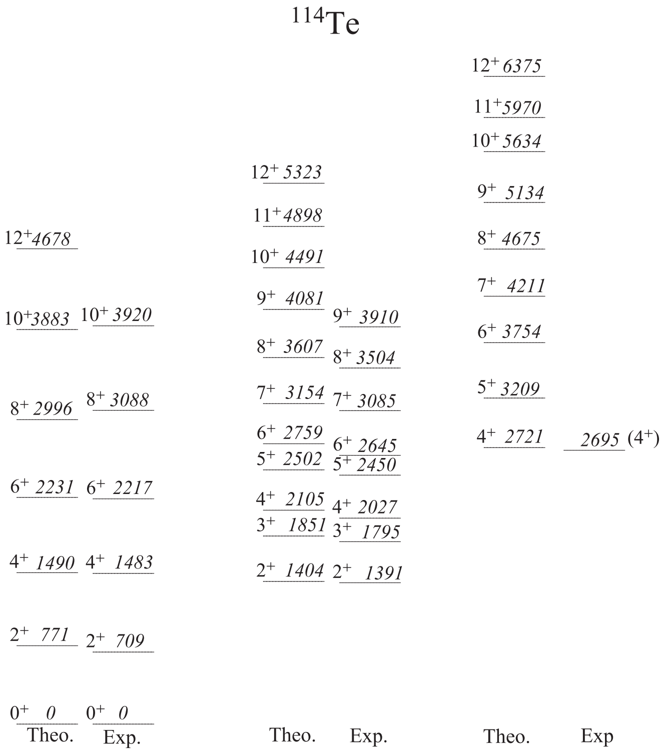

FIG. 12. Comparison of experimental and calculated band energies using the TPSM formalism in ^{114}Te. The level energies associated with the states are given in keV.

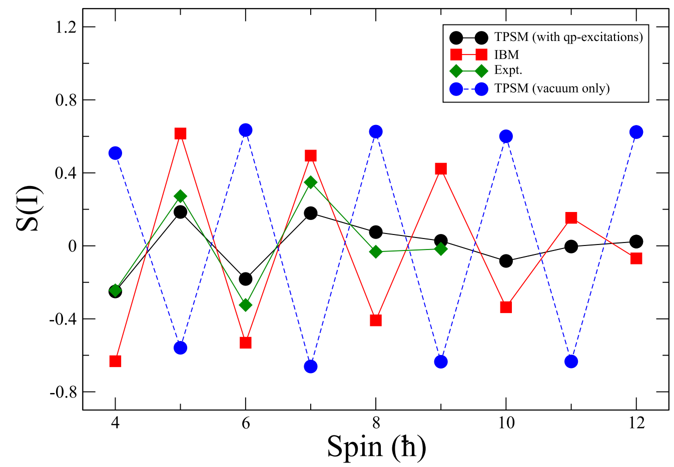

FIG. 13. Comparison of observed, TPSM, and IBM calculated staggering parameter, Eq. (8), for the quasi-γ band in ^{114}Te. The TPSM solid curve (black color) is with quasiparticle excitations and the dotted curve (blue color) is with vacuum only.

B. Triaxial projected shell model calculation

The multiquasiparticle TPSM approach has been developed and it has been shown to provide a consistent description of yrast, γ $(K = 2)$, and $\gamma\gamma$ $(K = 4)$ bands in transitional nuclei [40,48,49]. In this method, the three-dimensional projection technique is employed to project out the good angular-momentum states from product states built upon quasiparticle configurations of the triaxially deformed Nilsson+BCS model. The shell model Hamiltonian is then diagonalized in this angular-momentum projected basis. The TPSM space includes multiquasiparticle states, hence it is capable of describing near-yrast band structures at high- spins.

The TPSM basis employed in this study consists of zero-quasiparticle (0-qp) vacuum, two-proton, two-neutron, and four-quasiparticle configurations [50]. The quasiparticle basis chosen is adequate to describe high-spin states up to angular momentum $I \approx 20$. In the present analysis, we shall, therefore, restrict our discussion to this spin regime.

As in the earlier TPSM calculations, we use the pairing plus quadrupole-quadrupole Hamiltonian [51]

$$\hat{H} = \hat{H}_0 - \frac{1}{2}\chi \sum_{\mu} \hat{Q}^{\dagger}_{\mu}\hat{Q}_{\mu} - G_M \hat{P}^{\dagger}\hat{P} - G_Q \sum_{\mu} \hat{P}^{\dagger}_{\mu}\hat{P}_{\mu}, \quad (7)$$

where $\hat{H}_0$ is the spherical single-particle Hamiltonian, which contains a proper spin-orbit force [52]. χ is the strength of the quadrupole-quadrupole force related in a self-consistent way to deformation of the quasiparticle basis and G_M and G_Q are the strengths of the monopole and quadrupole pairing terms, respectively. The configuration space employed corresponds to three principal oscillator shells $\nu[3, 4, 5]$ and $\pi[2, 3, 4]$. The pairing strengths have been parametrized in terms of two constants G_1 and G_2. In this work, we choose $G_1 =$ 21.14 MeV and $G_2 = 13.86$ MeV; with these pairing strengths we approximately reproduce the experimental odd-even mass differences in this region. The quadrupole pairing strength G_Q is assumed to be proportional to G_M, and the proportionality constant was set to 0.18. These interaction strengths are consistent with those used earlier for the same mass region [53–55].

TPSM calculations proceed in several stages. In the first stage, the deformed basis space is constructed by solving the triaxially deformed Nilsson potential. In the present work, the axial deformation parameter $\epsilon = 0.150$ was adopted from the Ref. [56]. The non-axial deformation parameter $\epsilon' = 0.09$ was chosen so that the behavior of the γ band is properly described.

In the second step, the good angular-momentum states are obtained from the deformed basis by employing the three-dimensional angular-momentum projection technique. The projected bands obtained from zero-, two-, and four-quasiparticle states close to the Fermi surface are displayed in Fig. 11, the so-called band diagram, which are the diagonal matrix elements before band mixing. The projection from the zero-quasiparticle configuration gives rise to band structures with $K = 0, 2, 4$, corresponding to the ground-state, γ, and $\gamma\gamma$ bands. The calculated bandhead energies of the γ and $\gamma\gamma$ bands are about 1.2452 and 2.7252 MeV, respectively, above the ground state.

In the third and the final stage, the projected bases are used to diagonalize the shell model Hamiltonian, Eq. (7). The band energies, obtained after diagonalization, are shown in Fig. 12 with the available experimental data. It is evident from the figure that TPSM results are in excellent agreement with the known experimental energies. In Fig. 12, the calculations slightly overestimate the bandhead energy of the $\gamma\gamma$ band,

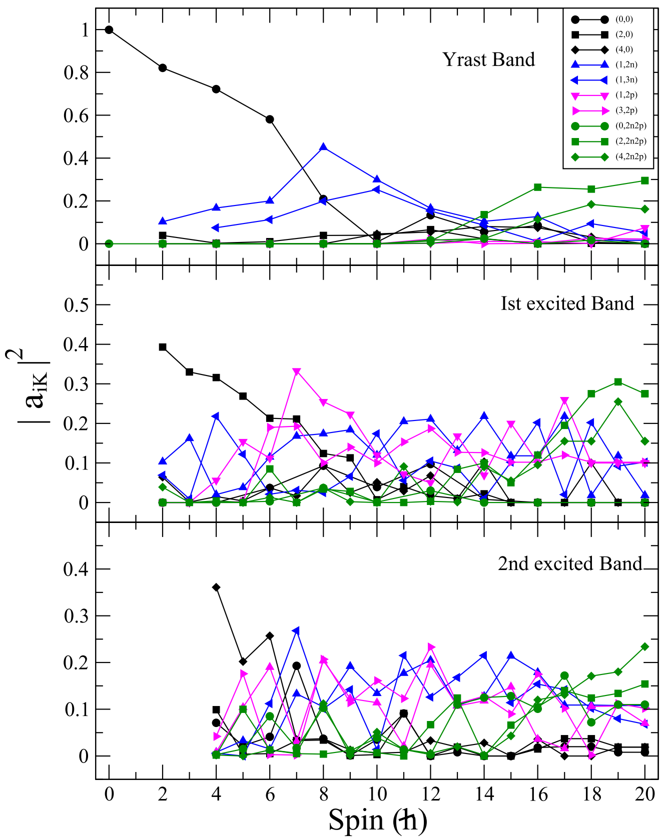

FIG. 14. Probabilities of the projected configurations in the yrast band and the first and second excited bands.

and we hope that this well-developed band will be populated in future experimental studies. The first quasiparticle $h_{11/2}{}^2$ two-neutron alignment is predicted around $I = 8$, and the transition to a four-quasiparticle $\nu(h_{11/2})^2\pi(g_{9/2})^2$ band is expected to occur around $I = 14$.

In order to understand the importance of the γ degree of freedom in the description of the triaxial shape in ^{114}Te, the staggering parameter, defined as,

$$S(I) = \frac{[E(I) - E(I-1)] - [E(I-1) - E(I-2)]}{E(2_1^+)}, \quad (8)$$

is plotted for the quasi-γ band in Fig. 13 with vacuum configuration only and with all the quasiparticle configurations. In the same figure, we also provide results of the IBM approach, which are good agreement with experimental data. It is evident from Fig. 13 that the phase of the staggering of the quasi-γ band with vacuum configuration only and that with the inclusion of the quasiparticle excitations are opposite to each other. The phase with the vacuum configuration only has odd-spin states lower than the even-spin states and corresponds to Davydov-Filippov or γ-rigid motion [57]. The inclusion of the quasiparticle excitations is shown to reverse the staggering phase with even-spin states lower than the odd-spin states as in the limiting case of Wilet-Jean or γ-soft motion [2]. Therefore, the inclusion of the quasiparticle excitations transforms the motion from γ rigid to γ soft. The phase and the magnitude of the staggering after the inclusion of the quasiparticle excitations is in good agreement with the corresponding experimental numbers and, therefore, it can state that the ^{114}Te nucleus is γ soft. The TPSM results further indicate that above spin the staggering amplitudes become smaller, and the reason for this is due to a considerable mixing of the two-quasiparticle configurations with the quasi-γ band at higher spins. In order to probe the mixing, the probabilities of various projected configurations are plotted in Fig. 14 for the yrast band and the first and second excited bands. The yrast band up to $I = 6$ is dominated by the zero-quasiparticle configuration with (0,0), i.e., $K = 0$, and above this spin the two-neutron aligned band $[(1, 2n)]$ is the dominant configuration. Above $I = 14$, the yrast band is primarily composed of four-quasiparticle configurations $[(2, 2n2p)]$. The first excited band has the dominant $K = 2$ zero-quasiparticle configuration [(2,0)] until $I = 6$ and, therefore, is the γ band. However, above $I = 6$, the first excited band has two-quasiparticle dominant component $[(1, 2p)]$. The second excited band has a dominant $K = 4$ zero-quasiparticle configuration [(4,0)], referred to as the $\gamma\gamma$ band, up to $I = 6$. Above this spin value, mixed structures are obtained. The $(1, 2n)$, $(3, 2n)$, $(1, 2p)$, and $(3, 2p)$ states from the two-quasiparticle configuration seem to become important along with some four-quasiparticle configurations.

VI. SUMMARY

Excited states of ^{114}Te were populated by means of the light-ion induced fusion evaporation reaction ^{112}Sn(^{4}He, $2n$) ^{114}Te at 37 MeV beam energy. Several new γ transitions were placed in the level scheme of ^{114}Te, based on the γ-γ coincidence and relative intensity measurements. The spin and parity of the levels were assigned on the basis of angular correlation and polarization asymmetry measurements. Theoretical calculations under the framework of the triaxial projected shell model and interacting boson model were performed in order to interpret the experimental results. Both the model calculations were found to be in good agreement with the experimental results, thereby confirming the existence of the quasi-γ band structure in the ^{114}Te nucleus. Further, systematic experimental investigations of low-lying states are required in order to understand the shape evolution in Te isotopes.

ACKNOWLEDGMENTS

The authors gratefully acknowledge the effort of the cyclotron operators for providing a good quality of ^{4}He beam. We would like to thank all the members of INGA collaboration for their support and active involvement. INGA is partially funded by the Department of Science and Technology, Government of India (No. IR/S2/PF-03/2003-II). S.R. would like to acknowledge financial assistance from the University Grants Commission, Minor Research Project [No. PSW-249/15-16 (ERO)]. G.G. acknowledges the support provided by the University Grants Commission, Departmental Research Support (UGC-DRS) program. P.R. acknowledges the support of a UGC-NET fellowship (Sr. No. 2121551170).

H.P. is grateful for the support of a Ramanujan Fellowship research grant under SERB-DST (SB/S2/RJN-031/2016). H.P. is also grateful for the fruitful discussion with Prof. Sukalyan Chattopadhyay (SINP, Kolkata).

[1] A. Bohr and B. R. Mottelson, *Nuclear Structure*, Vol. II (Benjamin, New York, 1975).
[2] L. Wilets and M. Jean, Phys. Rev. **102**, 788 (1956).
[3] R. K. Sheline, Rev. Mod. Phys. **32**, 1 (1960).
[4] H. Kusakari *et al.*, Nucl. Phys. A **242**, 13 (1975).
[5] P. E. Garrett and J. L. Wood, J. Phys. G **37**, 064028 (2010).
[6] P. E. Garrett *et al.*, Phys. Rev. C **86**, 044304 (2012).
[7] P. E. Garrett *et al.*, EPJ Web Conf. **66**, 02039 (2014).
[8] P. E. Garrett *et al.*, J. Phys. G **43**, 084002 (2016).
[9] C. M. Petrache *et al.*, Phys. Rev. C **99**, 024303 (2019).
[10] M. Spieker, P. Petkov, E. Litvinova, C. Muller-Gatermann, S.G. Pickstone, S. Prill, P. Scholz, and A. Zilges, Phys. Rev. C **97**, 054319 (2018).
[11] P. E. Garrett *et al.*, Phys. Rev. Lett. **123**, 142502 (2019).
[12] S. Chakraborty *et al.*, Nucl. Phys. A **996**, 121687 (2020).
[13] M. Saxena, R. Kumar, A. Jhingan, S. Mandal, A. Stolarz, A. Banerjee, R. K. Bhowmik, S. Dutt, J. Kaur, V. Kumar, M. Modou Mbaye, V. R. Sharma, and H. J. Wollersheim, Phys. Rev. C **90**, 024316 (2014).
[14] S. S. Tiwary *et al.*, Eur. Phys. J. A **55**, 163 (2019).
[15] J. J. Van Ruyven and J. L. Wood, Nucl. Phys. A **380**, 125 (1982).
[16] R. F. Casten, Nat. Phys. **2**, 811 (2006).
[17] E. A. McCutchan, D. Bonatsos, N. V. Zamfir, and R. F. Casten, Phys. Rev. C **76**, 024306 (2007).
[18] N. V. Zamfira and R. F. Casten, Phys. Lett. B **260**, 265 (1991).
[19] T. Lönnroth, A. Virtanen, and J. Hattula, Phys. Scr. **34**, 682 (1986).
[20] C.-B. Moon *et al.*, Phys. Rev. C **51**, 2222 (1995).
[21] I. Thorslund *et al.*, Phys. Rev. C **52**, R2839 (1995).
[22] R. B. Cakirli, R. F. Casten, J. Jolie, and N. Warr, Phys. Rev. C **70**, 047302 (2004).
[23] O. Möller, N. Warr, J. Jolie, A. Dewald, A. Fitzler, A. Linnemann, K.O. Zell, P. E. Garrett, and S. W. Yates, Phys. Rev. C **71**, 064324 (2005).
[24] C. Qi, Phys. Rev. C **94**, 034310 (2016).
[25] H. Pai *et al.*, Vacuum **167**, 393 (2019).
[26] S. Bhattacharya *et al.*, Proc. DAE Symp. Nucl. Phys. **63**, 1156 (2018).
[27] S. Das *et al.*, Nucl. Instrum. Methods Phys. Res. A **893**, 138 (2018).
[28] S. Chatterjee *et al.*, Proc. DAE Symp. Nucl. Phys. **63**, 1100 (2018).
[29] D. C. Radford, Nucl. Instrum. Methods Phys. Res. A **361**, 297 (1995).
[30] R. Bhowmik *et al.*, Proc. DAE Symp. Nucl. Phys. **44B**, 422 (2001).
[31] A. Krämer-Flecken *et al.*, Nucl. Instrum. Methods Phys. Res. A **275**, 333 (1989).
[32] E. S. Macias *et al.*, Comput. Phys. Commun. **11**, 75 (1976).
[33] K. Starosta *et al.*, Nucl. Instrum. Methods Phys. Res. A **423**, 16 (1999).
[34] Ch. Droste *et al.*, Nucl. Instrum. Methods Phys. Res. A **378**, 518 (1996).
[35] H. Pai *et al.*, Phys. Rev. C **85**, 064313 (2012).
[36] P. Van Nes *et al.*, Nucl. Phys. A **379**, 35 (1982).
[37] J. Blachot, Nucl. Data Sheets **113**, 515 (2012).
[38] B. E. Zimmerman, The energy level structures of even-even tellurium and odd-odd iodine and antimony nuclei: ^{114}Te, ^{116}Te, ^{114}I, and ^{114}Sb, Ph.D. thesis, University of Maryland, 1992 (unpublished).
[39] A. Guessous *et al.*, Phys. Rev. Lett. **75**, 2280 (1995).
[40] S. Chakraborty *et al.*, Eur. Phys. J. A **55**, 46 (2019).
[41] J. M. Sears, D. B. Fossan, G. R. Gluckman, J. F. Smith, I. Thorslund, E. S. Paul, I. M. Hibbert, and R. Wadsworth, Phys. Rev. C **57**, 2991 (1998).
[42] C. B. Moon *et al.*, Nucl. Phys. A **510**, 173 (1990).
[43] H. Watanabe *et al.*, Phys. Lett. B **704**, 270 (2011).
[44] A. K. Singh, G. Gangopadhyay, and D. Banerjee, Phys. Rev. C **53**, 2524 (1996); **55**, 968 (1997).
[45] G. L. Long, S. J. Zhu, and H. Z. Sun, J. Phys. G **21**, 331 (1995).
[46] D. Bonatsos, *Interacting Boson Models of Nuclear Structure* (Clarendon, Oxford, 1988).
[47] E. A. McCutchan, N. V. Zamfir, and R. F. Casten, Phys. Rev. C **69**, 064306 (2004).
[48] J. A. Sheikh and K. Hara, Phys. Rev. Lett. **82**, 3968 (1999).
[49] Y. Sun, K. Hara, J. A. Sheikh, J. G. Hirsch, V. Velazquez, and M. Guidry, Phys. Rev. C **61**, 064323 (2000).
[50] J. A. Sheikh, G. H. Bhat, Y. Sun, G. B. Vakil, and R. Palit, Phys. Rev. C **77**, 034313 (2008).
[51] K. Hara and Y. Sun, Int. J. Mod. Phys. E **4**, 637 (1995).
[52] S. G. Nilsson, C. F. Tsang, A. Sobiczewski, Z. Szymanski, S. Wycech, C. Gustafson, I. Lamm, P. Moller, and B. Nilsson, Nucl. Phys. A **131**, 1 (1969).
[53] G. H. Bhat, W. A. Dar, J. A. Sheikh, and Y. Sun, Phys. Rev. C **89**, 014328 (2014).
[54] C. L. Zhang, G. H. Bhat, W. Nazarewicz, J. A. Sheikh, and Y. Shi, Phys. Rev. C **92**, 034307 (2015).
[55] J. A. Sheikh, G. H. Bhat, R. Palit, Z. Naik, and Y. Sun, Nucl. Phys. A **824**, 58 (2009).
[56] P. Möller *et al.*, At. Data Nucl. Data Tables **59**, 185 (1995).
[57] A. S. Davydov and G. F. Filippov, Nucl. Phys. **8**, 237 (1958).